NASA TECHNICAL NOTE

NASA TN D-5613

c. 1

NASA TN D-5613

CORRELATION ANALYSIS AND SCINTILLATION FOR 15-GHz LINE-OF-SIGHT PROPAGATION CHANNELS

by E. Mondre

Goddard Space Flight Center
Greenbelt, Md. 20771

NATIONAL AERONAUTICS AND SPACE ADMINISTRATION • WASHINGTON, D. C. • APRIL 1970

1. Report No.	2. Government Accession No.	3. Recipient's Catalog No.
NASA TN D-5613		

4. Title and Subtitle

Correlation Analysis and Scintillation for 15-GHz Line-of-Sight Propagation Channels

5. Report Date: April 1970

6. Performing Organization Code

7. Author(s): E. Mondre

8. Performing Organization Report No.

9. Performing Organization Name and Address

Goddard Space Flight Center
Greenbelt, Maryland 20771

10. Work Unit No.

11. Contract or Grant No.

12. Sponsoring Agency Name and Address

National Aeronautics and Space Administration
Washington, D. C. 20546

13. Type of Report and Period Covered: Technical Note

14. Sponsoring Agency Code

15. Supplementary Notes

16. Abstract

Experiments have been carried out to measure the temporal nature of amplitude fluctuations under various weather conditions observed on a 15-GHz line-of-sight propagation channel. The path length is on the same order as the atmospherically influenced portion of an earth-spacecraft link which will allow direct comparison with data to be obtained from the ATS-E Millimeter Wave Propagation Experiment. Mean value, mean square value, and statistics of amplitude fluctuations are computed. It is concluded that a Rician distribution is adequate to describe the amplitude data. Channel correlation analysis is discussed. The computed echo correlation functions and echo power spectral densities indicate a channel coherence time of 1.5 to 4 seconds and a fading bandwidth of less than 0.4 Hz. Magnitudes and spectral densities of amplitude scintillations are calculated from the experimental data and compared with theoretical results derived from the turbulence of the atmosphere.

17. Key Words Suggested by Author	18. Distribution Statement
	Unclassified - Unlimited

19. Security Classif. (of this report)	20. Security Classif. (of this page)	21. No. of Pages	22. Price*
Unclassified	Unclassified	16	$3.00

*For sale by the Clearinghouse for Federal Scientific and Technical Information
Springfield, Virginia 22151

CONTENTS

CORRELATION ANALYSIS AND SCINTILLATION FOR 15-GHz LINE-OF-SIGHT PROPAGATION CHANNELS*

by
E. Mondre
Goddard Space Flight Center

INTRODUCTION

Propagation studies of millimeter waves through the atmosphere are of concern both to communication applications and to investigations of the atmospheric structure. Most of the published results refer to long-term statistics of gaseous absorption and attenuation due to precipitation (References 1, 2, 3, and 4). There is a need for quantitative observation of short-term parameters such as correlation functions and the power spectral densities of the scintillations occurring on a line-of-sight path. These short-term statistical parameters allow a description of the time- and frequency-selective fading properties of a communication channel. In theoretical papers, discussing error probability, intermodulation distortion (References 5 and 6) and optimal demodulation of analog signals (Reference 7), the assumption is made that channel characteristics can be accurately estimated.

The millimeter-wave propagation experiment through the atmosphere between ATS-E spacecraft and various ground stations throughout the United States will yield information about the feasibility of using such frequencies for communication links. The planned data reduction for this experiment includes long-term statistics of signal attenuation as well as channel characterization with correlation functions and spectral densities. The latter is referred to as *short-term analysis*. The amplitude of the received signal will not be a stationary variable if observed over a very long period (hours or days, for example). However, when observed over a short time (a few minutes) the observable quantities will, in general, be stationary and thus the system can be considered quasi-stationary. One has, in effect, a quasi-wide-sense stationary uncorrelated scattering channel (References 8 and 9). It is the purpose of this report to discuss the short-term analysis based on experimental data obtained from a short line-of-sight link.

EXPERIMENTAL ARRANGEMENT

The path selected for the short-term analysis of a 15-GHz signal is over a distance of 4.6 km between a water tower in the Agricultural Research Center and Building 22 at Goddard Space

*This work was accomplished while the author held a National Research Council Postdoctoral Resident Research Associateship supported by National Aeronautics and Space Administration.

Flight Center. The length of the ground path is on the same order as that portion of a ground-spacecraft link which is influenced by atmospheric water vapor and oxygen as well as precipitation.

The transmitting antenna is mounted at a height of approximately 30 meters on the water tower. The focal-point-fed paraboloid with 1.2-meter diameter has a nominal gain of 43 db and a half power beam width in the E-plane of 1.05 degree. Vertical polarization is employed throughout the experiment. The 15-GHz power source is a Varian Klystron with 760-milliwatt power output.

On the receiving site at the roof of Building 22 (18 meters above ground) a horn antenna with an aperture of 40 cm^2 (nominal gain 19.5 db) is implemented. The signal is detected with a balanced mixer and a 30-MHz phase-lock loop receiver. The output of the receiver is recorded on a strip chart recorder operating at a chart speed of 1 mm/sec and also on an FM magnetic tape recorder. The profile of the ground along the path is fairly flat. Clearance of the line-of-sight path with respect to any natural obstacles is good. Note that in general the path and antenna alignments preclude ground reflection.

Power and frequency instabilities of the klystrons are negligible since short-term analysis of atmospheric scintillations is the main goal of this experiment. During each of the short data runs (four minutes) power and frequency did not change. The receiver is calibrated on a clear day with low humidity with the aid of a calibrated attenuator.

Rain data are collected at five points along the path. The rain gauges are spaced at approximately equal distances (separation varies from 970 to 1240 meters). The resolution of the tipping buckets is 0.01 inch/tip. In determining the average rainfall rate along the path it is assumed that the indicated rate at a particular gauge applies over half the distance to the adjacent gauges.

DATA RECORDING

Data records are collected over a two-month interval (June and July). Selected samples for different atmospheric parameters (humidity, rain, wind) are used for data analysis. Two extreme cases are shown in Figure 1. Sample A is recorded on a clear day with few clouds, an average water-vapor concentration of 10 gr/m^3, and a temperature of 70°F. Record B is a sample taken during a rainstorm with a rainfall rate of 32 mm/hr, a water-vapor concentration of 17 gr/m^3, and an average temperature of 76°F. Record C is taken on a hot day (92°F) with a water-vapor concentration of 16.5 gr/m^3. The wind speed perpendicular to the path is approximately 11 km/hr for records A and B, and 20 km/hr for record C.

The data on the analog magnetic tape are used in connection with a special-purpose multichannel data processor built by Federal Scientific Corporation for the ATS-E Millimeter Wave Propagation Experiment. This processor can be used to determine correlation functions and spectra of the data records. (Details are discussed later.) However, the main part of the data analysis is performed on an IBM 360 digital computer. Therefore, the recorded data are played back through an analog-to-digital converter, to generate a digital data tape. The analog record is sampled at a 30-Hz rate for 4 minutes. Each of the digital data records therefore contains 7200 samples. The

record-time length for each data run is selected to provide a reasonable trade-off between the statistically time-varying propagation medium and the statistical reliability of the measurement.

The cutoff frequency due to sampling is 15 Hz, which is well above all the expected frequency components of the scintillation. Amplitude quantization is done in 224 steps over the range of ±1 volt. This gives a resolution in amplitude of about 9 mV. If a uniform probability distribution over one scale unit is assumed, the rms noise-to-signal ratio introduced by quantization is approximately 0.0013 (Reference 10).

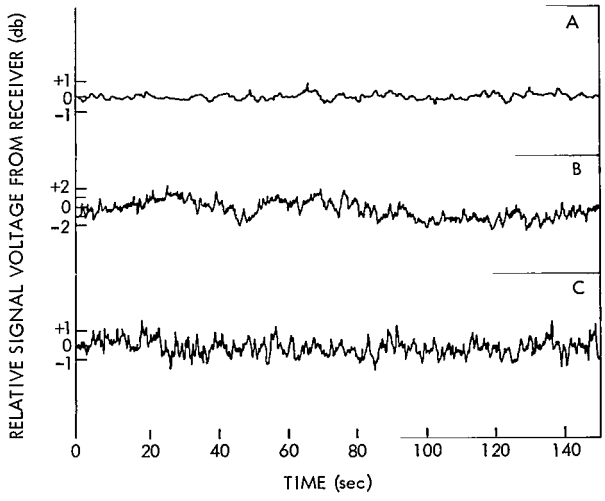

Figure 1—Samples of received signal amplitude.

STATISTICS OF SIGNAL FLUCTUATION

Test for Stationarity

It is important to test the data records for stationarity, since calculation of correlation function and spectrum is only useful for a channel which is at least a quasi-wide-sense stationary uncorrelated scattering channel (References 8 and 9). To test the stationarity of the data, the sample record is divided into 20 equal time intervals. The data in each interval may now be considered independent. Both mean value and mean square value are computed for each interval. They are compared with the mean value and mean square value for the whole data record length. A run test (Reference 10) is used to decide whether the hypothesis (data are stationary) is accepted or rejected. The test is performed at a 0.05 level of significance.

During one occurrence with heavy rain the record length must be reduced to 1.5 minutes to ascertain stationarity of the data. All other records, even those with rain and strong wind, are stationary over the 4-minute interval.

This test verifies weak stationarity since mean value and mean square value only are tested. But actual physical models are generally also strongly stationary if they are weakly stationary. In the case of data with a Gaussian probability density function, weakly stationary data are automatically strongly stationary. It is shown later that the expected Rician fading statistics can be approximated by a Gaussian distribution with nonzero mean.

Signal Attenuation

The mean signal level is calculated for each data run from

$$\bar{x} = \frac{1}{N} \sum_{i=1}^{N} x_i , \qquad (1)$$

where N is the number of samples, and x_i are individual record samples. For data runs taken on humid days (water-vapor concentration between 10 and 30 gr/m^3) the mean value is approximately 0.09 to 0.22 db/km below the dry-day level. This agrees with the reported values of 0.006 to 0.01 db/km per gr/m^3 for attenuation due to water vapor (References 11 and 1).

Data runs during precipitation are made in drizzle and rain with average rainfall rates of 16.5 and 32 mm/hr. The readings of individual buckets during the heavy rain occurrence were not the same, thus indicating a spatial inhomogeneity along the path. The bucket readings varied from 2 to 20 tips during a 5-minute period. The theoretical attenuation is calculated from the empirical relation

$$A = a\bar{R}^b \tag{2}$$

where A is the attenuation in db/km, $\bar{R}$ the average rainfall rate in mm/hr, and a and b are parameters. Numerical values for these two parameters can be found in the literature (References 3, 4, 12, and 13). At a frequency of 15 GHz, suitable values seem to be $a = 0.035$ and $b = 1.155$. For the two reported rain occurrences we find attenuations of 0.9 and 1.92 db/km. The measured signal attenuation during these two events gives 0.9 and 2 db/km, which is in good agreement with the calculated values. This does not prove that the chosen values for parameters a and b will fit best for all rain events, since the attenuation depends in a very complex manner on the rainfall rate (drop-size distribution and rain intensity). The best choice for a and b can only be made from data collected over a long period during different rain events. But this is not within the scope of this paper.

The calculated mean values are used to transform the data to have zero mean value. This is done in order to simplify subsequent formulas and improve the accuracy of the calculations. The data can now be converted into the ratio of received electric field to mean electric field by means of the receiver calibration curve. In the vicinity of the mean value the calibration curve is approximated by a straight line. The mean value m of the electric-field ratio E/E_0 is obviously equal to one.

Signal Statistics

The propagation channel can be described by theoretical models, a procedure that allows the determination of the expected probability density function for the received signal amplitude. The simplest model with the output of the channel a Gaussian random process leads to a Rayleigh distribution of the envelope-detected signal. This model is usually not correct for line-of-sight propagation where a strong coherent (direct) signal is received. If the coherent signal is added to the Gaussian model, the envelope of the received signal will have a Rician statistic (Reference 14). Another model generally used in laser propagation studies assumes a logarithmic-normal (log-normal) distribution for the signal amplitude. This means that the logarithm of the received envelope (or envelope expressed in db) is normally distributed.

Rician and log-normal distributions are described by two parameters each, which can be calculated from the mean value and mean square value of the recorded data (Reference 15). Note that

the Rayleigh distribution is defined by one parameter only. It can be shown that in this case the ratio of mean value and standard deviation is constant and equal to

$$\frac{m}{\sigma} = \left(\frac{\pi}{4-\pi}\right)^{1/2} = 1.92 . \qquad (3)$$

All the data records have a ratio m/σ greater than 25, which excludes, as expected, the Rayleigh distribution. For such large ratios of coherent and fading components, the Rician distribution can be approximated by a Gaussian distribution with nonzero mean (Reference 16).

The probability density function for both models (Rician and log-normal) is computed for each data record. Figure 2 shows an example of the theoretical probability density for sample record B. It can be seen that there is a negligible difference between these two distributions, as is expected for such large ratios of steady and fading components. Figure 2 also shows the probability density calculated from record B, which is not unique because it is determined by the choice of the number of class intervals in which the whole range is divided (Reference 10). These are shown as "X"-marks in the figure.

Figure 3 shows examples of the distribution function plotted on Gaussian probability paper. Again the Rician and log-normal distributions, as well as the experimental data, are plotted. The values at the "tails" of the distribution

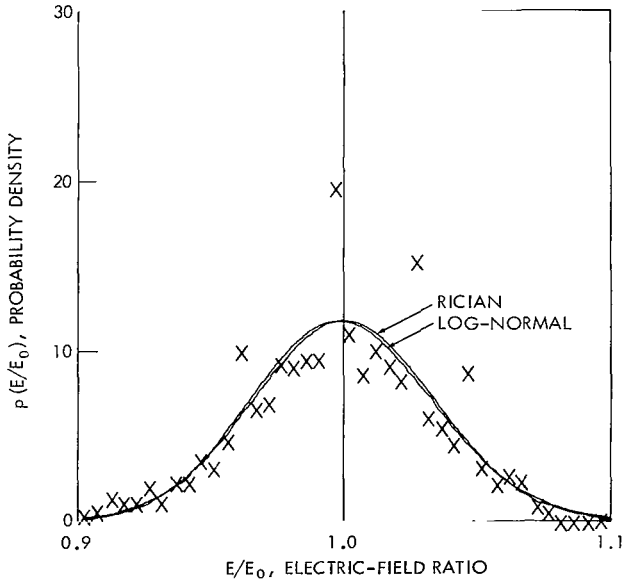

Figure 2—Probability density function of received electric-field for record B.

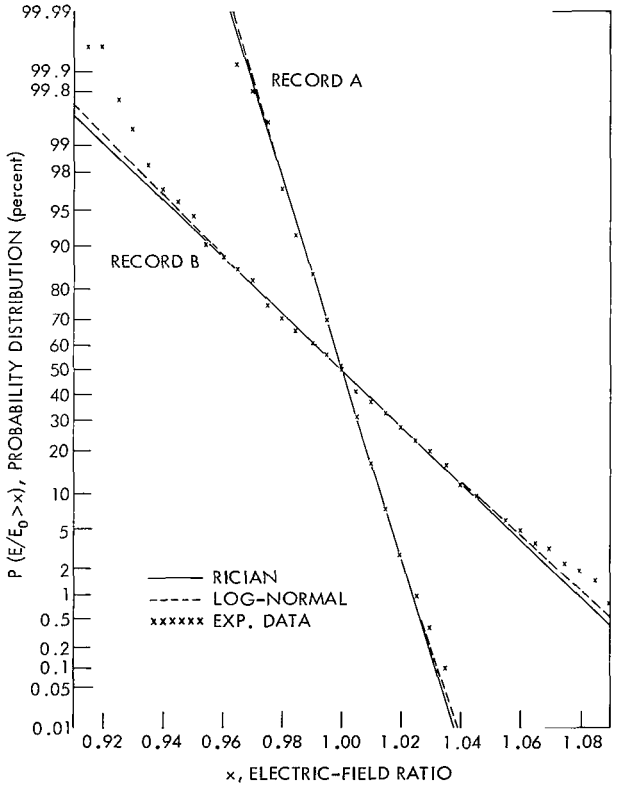

Figure 3—Rician, log-normal, and measured probability distribution.

function are statistically uncertain owing to the finite sample size. The "tail" values are derived from only a few data points; one additional data point falling into these intervals would cause a noticeable change in the distribution function. All data records can be classified as having either Rician or log-normal envelope density.

Signal Scintillation

Scintillation of the received signal is caused by fluctuation of the dielectric constant of the atmosphere. As already pointed out, ground reflections, which also would produce amplitude fading, are not to be expected. The standard deviation σ can be calculated from

$$\sigma = \left[\frac{1}{N}\sum_{i=1}^{N} x_i^2\right]^{1/2}, \tag{4}$$

where x_i are the transformed data values (electric-field ratios) with zero mean. For clear sky and calm wind the standard deviation of the field fluctuations ranges from 1 to 2 percent of the mean value, and goes up to 3.5 percent for heavy rain and wind velocities on the order of 20 km/hr.

Since the amplitude is approximately a Gaussian distributed variable (see Figure 3), the probability that the instantaneous signal level will be between $+3\sigma$ and -3σ of its average level is 99.7 percent. With this confidence level, the maximum scintillation of the signal amplitude in percent of the mean signal level is given by

$$\Delta\alpha = \pm\frac{3\sigma}{m}\,100, \tag{5}$$

where $m = 1$ and σ is defined in Equation 4. The maximum scintillation is calculated for all recorded data runs. The absolute values for $\Delta\alpha$ are between 3 and 10 percent.

Tatarski (Reference 17) developed a turbulence theory where the atmospheric turbulence is described by a "structure function." The structural constant in this structure function, denoted by C_n, is related to the variance of the logarithm of the signal amplitude by

$$\sigma_{\chi}^2 = 0.31\, C_n^2\, k^{7/6}\, L^{11/6} \tag{6}$$

for $\ell_0 \ll \sqrt{\lambda L} \ll L_0$, where L is the path length and $k = 2\pi/\lambda$ the spatial wave number (λ = wavelength). L_0 is the outer scale of the turbulence (largest "blob" size). Close to ground it is often assumed that the outer scale is on the order of the beam height above ground. Near the ground, the inner scale ℓ_0 is on the order of several millimeters. Equation (6) is derived on plane-wave assumption (Reference 17).

Although the condition $L_0 >> \sqrt{\lambda L}$ is not exactly satisfied ($L_0 \sim 20$-25 m, $\sqrt{\lambda L} = 9.6$ m), values for C_n are calculated from the measured signal fluctuation by means of Equation (6) and the definition of the variance of the logarithmic amplitude

$$\sigma^2_{\ell_n} = \overline{(\ell n\, E/E_0)^2}\,. \tag{7}$$

Since E/E_0 is approximately log-normal distributed, the quantity $\sigma^2_{\ell_n}$ can be derived from the already computed variance of the signal amplitude σ^2, according to

$$\sigma^2_{\ell_n} = \ell n\left(1 + \sigma^2/m^2\right)\,. \tag{8}$$

The structural constant C_n is found to vary between 0.28×10^{-6} and 0.93×10^{-6} $m^{-1/3}$. Reported values for C_n obtained from measurements of fluctuations in phase differences and direct measurements to the refractive index and temperature spectra in the troposphere vary over a wide range from 0.019×10^{-6} to 0.98×10^{-6} $m^{-1/3}$ (Reference 18).

The maximum expected scintillation for a link through the entire atmosphere can be estimated if different models are assumed for the structural constant as a function of height. Tatarski's theory gives the relation

$$\sigma^2_{\ell_n} = \gamma\, C^2_{n0}\, k^{7/6} \left(h_0 \sec\beta\right)^{11/6}\,, \tag{9}$$

where C_{n0} is the value of C_n at the Earth's surface, and h_0 is assumed to be 2000 m or 3200 m. The first value corresponds to the results of soundings with a balloon-borne refractometer (Reference 19). The direction of the propagation link is defined by the zenith angle β. The factor γ depends on the assumed model. Values of γ are shown in Table 1 (Reference 17).

With Equations (5), (8), and (9) we obtain the expected maximum amplitude fluctuations summarized in Table 2. We calculate C_{n0} from the measured maximum value of $C_n = 0.93 \times 10^{-6}$ $m^{-1/3}$ at an average beam height of 25 meters. A zenith angle of $\beta = 48°30'$ corresponds to the look angle from the ATS-E ground station at Rosman, North Carolina, to the ATS-E spacecraft in synchronous orbit at 108°W longitude.

Table 1

Values of γ for Different Models for Structural Constant.

Model		γ
1	$C_n^2 = C_{n0}^2 \exp\left(-h/h_0\right)$	0.53
2	$C_n^2 = C_{n0}^2 \left[1 + \left(h/h_0\right)^2\right]^{-1}$	3.4

Table 2

Expected Scintillation for Earth-Spacecraft Link (15 GHz).

Zenith Angle β	Model 1		Model 2	
	h_0 = 2000 m	3200 m	2000 m	3200 m
0°	±6.2%	±9.6%	±15.7%	±24.3%
48°30'	±9.1%	±14.0%	±23.0%	±35.0%

$C_n = 0.93 \times 10^{-6}\ m^{-1/3}$ at h = 25 m.

CHANNEL CORRELATION ANALYSIS

The time- and frequency-selective fading properties of a communication channel can be characterized from the correlation function of a test signal (References 8 and 9). In this experiment only a single frequency is used; thus only the echo correlation function and its Fourier transform—the echo power spectrum—can be calculated. This leads to information about the coherence time and fading bandwidth of the radio channel. Two other parameters of interest are the coherence bandwidth and time spread of the channel. To measure those parameters we must transmit two carriers and evaluate the cross-correlation function as a function of their frequency separation. This is planned for the ATS-E Millimeter Wave Propagation Experiment.

Echo Correlation Function

The echo correlation function is calculated from

$$R(\tau) = R(rh) = \frac{1}{N-r}\sum_{i=1}^{N-r} x_i\, x_{i+r} \qquad \left(r = 0, 1, 2 \cdots n\right), \qquad (10)$$

where r is the lag number and h the sampling interval which is 1/30 second. The sample data x_i are the transformed data with zero mean. It is very important to transform the data to zero mean before calculating the correlation function, in order to achieve accurate correlation function estimates. This is especially true if the mean value of the data is large compared with their standard deviation. For comparison it is better to use the covariance function rather than the correlation function. Dividing $R(\tau)$ by $R(0)$ gives the echo covariance function, which is shown in Figure 4 for different meteorological conditions.

The echo correlation function is calculated from the envelope-detected signal rather than the complex signal amplitude. A relationship between envelope and complex covariance for Rician envelope statistics is derived in Reference 15. As already pointed out, the ratio between coherent and random signal is very large. Therefore the calculated envelope covariance is indistinguishably close to the magnitude of the complex covariance (see Reference 15).

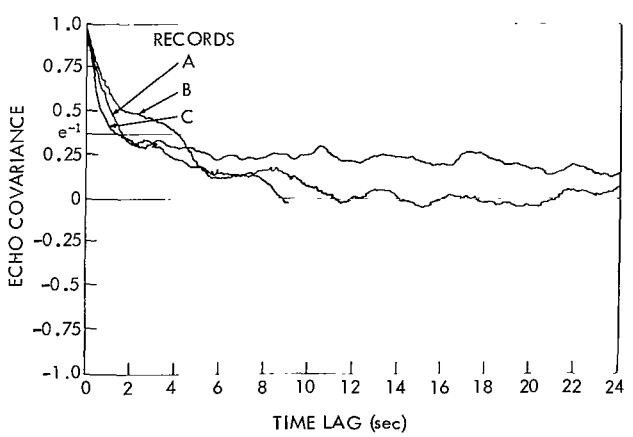

Figure 4—Echo covariance function of signal amplitude.

The *coherence time* T_c of the channel is defined in the literature as the interval in time lag τ over which $R(\tau)$ is essentially nonzero. This definition of T_c is useful from a theoretical point of view but it is usually not possible to calculate the correlation function with an accuracy for time lags great enough, to apply this definition.

For comparison and as a measure of T_c (T_c is used in an order-of-magnitude sense only) we approximate $R(\tau)/R(0)$ with the exponential function $\exp(-\tau/T_c)$, and redefine T_c in terms of this relation. It can be seen from Figure 4 that T_c is on the order of 1.5 to 4 seconds. For a physical interpretation of the coherence time one can think of T_c as a measure of the average duration of fades on the channel. In transmitting digital data, the duration of a symbol should be considerably less than T_c to allow for coherent integration of the received signal.

Echo Power Spectral Density

The power spectral density is obtained from the auto-correlation function by means of the Fourier transform. Owing to the finite sample size of the data records, only an estimate of the spectrum can be calculated. The auto-correlation function and power spectral density are, formally at least, even functions. Hence, the relation between those two functions may be expressed in the simpler form of the one-sided cosine transform, namely

$$\tilde{S}(f) = 2\int_0^\infty R(\tau)\cos(2\pi f\tau)\,d\tau\,. \tag{11}$$

A "raw" estimate of the true power spectral density is defined for an arbitrary f in the range $0 \le f \le f_c$ by

$$\tilde{S}(f) = 2h\left[R(0) + 2\sum_{r=1}^{n-1} R(rh)\cos\frac{\pi r f}{f_c} + R(nh)\cos\frac{\pi n f}{f_c}\right], \tag{12}$$

where $f_c = 1/2h$ is the cutoff frequency and $n \le N/10$. The spectrum is calculated for discrete frequencies $f_k = kf_c/n$, with $k = 0, 1, 2 \cdots n$.

A final smooth estimate of the power spectral density may be obtained by frequency smoothing, which is performed by multiplying the auto-correlation function by suitable even functions of τ. This amounts to weighting the correlation function nonuniformly. One way is to use the Hanning lag window weighting function, defined by

$$D_r = D(rh) = \begin{cases} \frac{1}{2}\left(1 + \cos\frac{\pi r}{n}\right) & r = 0, 1, \cdots n \\ 0 & r > n. \end{cases} \tag{13}$$

If time is discrete and computation digital, the smoothing can be done more economically in the frequency domain by transformation of the correlation function followed by convolution. Because $D(rh)$ are finite sums of constants and cosines, so that their transforms are simple sums of Dirac delta functions with appropriate spacing, convolution means only multiplying with weights 0.25,

0.5, 0.25; viz.:

$$S_0 = S(0) = 0.5\tilde{S}_0 + 0.5\tilde{S}_1 ,$$

$$S_k = S\left(k\frac{f_c}{n}\right) = 0.25\tilde{S}_{k-1} + 0.5\tilde{S}_k + 0.25\tilde{S}_{k+1} \qquad (k = 1, 2, \cdots n-1) ,$$

$$S_n = S(f_c) = 0.5\tilde{S}_{n-1} + 0.5\tilde{S}_n . \qquad (14)$$

Spectral distribution of the fluctuations indicate that for 15 GHz the scintillations are usually confined to frequencies less than 0.5 Hz. Figure 5 shows typical normalized echo power spectral densities obtained from the correlation functions of Figure 4. They are normalized with the square of the mean value. The ordinate in Figure 5 is the ratio of fluctuation power density and mean power. Plotted are the two extreme conditions A and B (see Figure 1) with standard deviations of 0.01 and 0.034. Also plotted is the spectrum of record C with a standard deviation of 0.025.

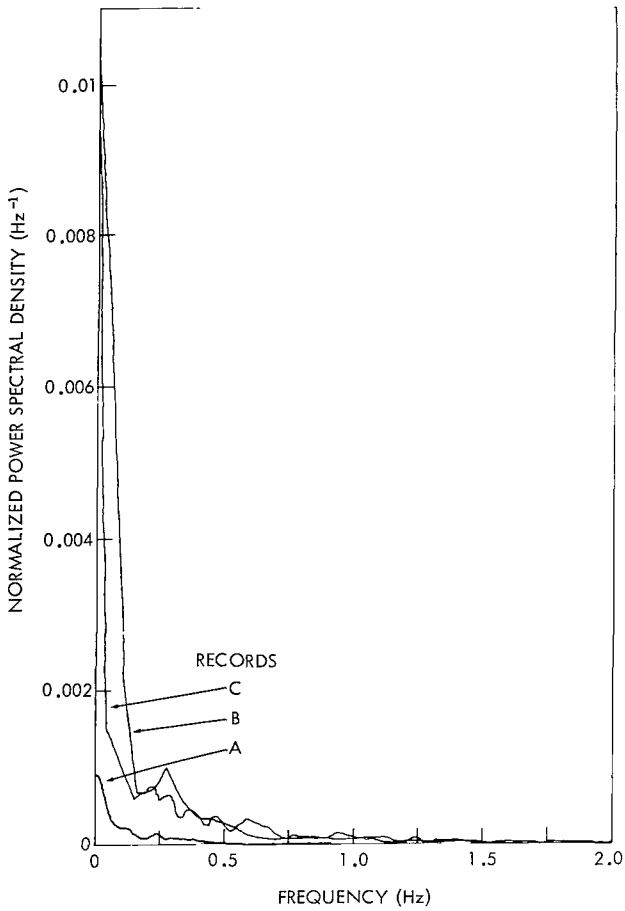

Figure 5—Echo power spectral density of amplitude fluctuations (normalized with mean d.c. power).

Since the total fluctuation power P_{ac} is equal to the variance σ^2, that is

$$\int_0^\infty S(f)\,df = \frac{P_{ac}}{P_{dc}} = \frac{\sigma^2}{m^2} \qquad (15)$$

($S(f)$ is normalized with square of the mean value), we may normalize the power spectral density by multiplying the plots in Figure 5 by m^2/σ^2. This leads to a presentation where the area under each curve is equal to one. As shown in Figure 6, all data records show a very similar power spectral density. The ordinate is now the ratio of fluctuation power density to total fluctuation power.

The fading bandwidth of the 4.6 km communication channel is approximately 0.4 Hz and does not seem to change very much with weather conditions.

It is interesting to compare the power spectral density with the theoretically expected spectrum derived from the spatial correlation and atmospheric structural functions. According to

Reference 18 the spectrum of the amplitudinal fluctuations is described by

$$S(f) = 0.016\, C_n^2\, k^2 L f^{-8/3} v_T^{5/3} , \qquad (16)$$

where v_T is the component of the mean wind speed normal to the path. This equation is valid for frequencies $f > v_T/\sqrt{\lambda L}$ whereas for $f < v_T/\sqrt{\lambda L}$ the spectrum is expected to be nearly constant.

Figures 7 and 8 show examples of the measured as well as the theoretical spectrum for data records A and C. In Figure 7 there is good agreement for f/v_T less than 0.5 m^{-1} (f = 1.5 Hz). The deviation for $f/v_T > 0.5$ is due to noise. The fluctuation power is concentrated in

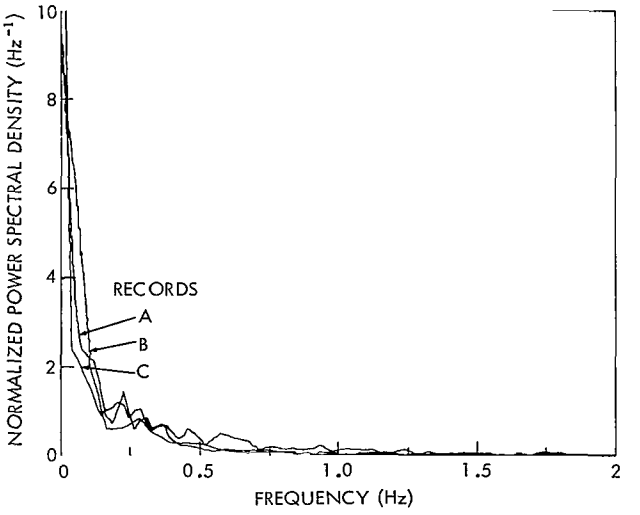

Figure 6—Echo power spectral density of amplitude fluctuations (normalized with total fluctiation power).

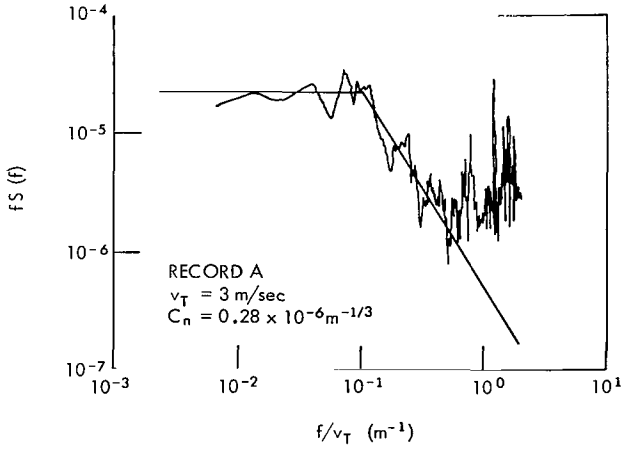

Figure 7—Normalized spectrum of amplitude fluctuation for record A.

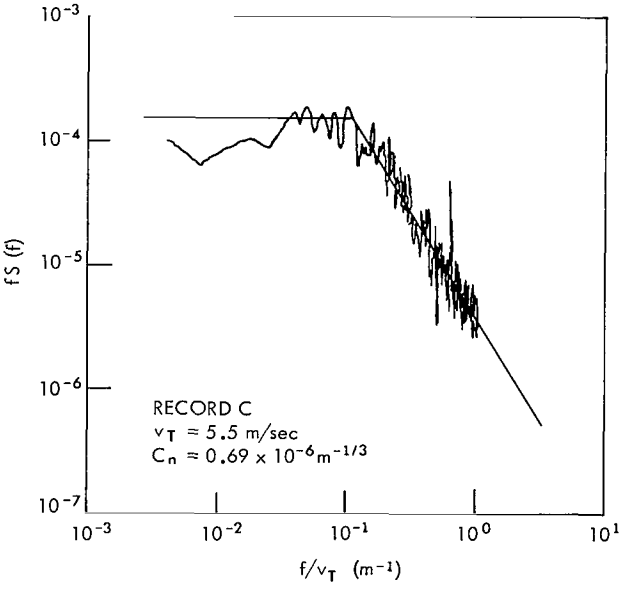

Figure 8—Normalized spectrum of amplitude fluctuation for record C.

frequencies below 0.5 Hz; therefore for higher frequencies the noise contribution predominates. Assuming white noise, the theoretical curve in Figure 7 should have a +45-degree slope for higher frequencies. The fluctuation power for record C is well above noise level for frequencies up to 6 Hz, as can be seen in Figure 8.

Analog Correlation Analysis

For comparison, the channel correlation analysis is also carried out on a special-purpose multi-channel data processor built by Federal Scientific Corporation for the ATS-E Millimeter Wave Propagation Experiment. A description of this processor is given in Reference 20. As input for the data processor, the analog tape with the recorded receiver output voltage is used.

The auto-correlation functions are calculated from data records 153.6 seconds in length. The time lag of the correlation function is from 0 to 102.4 seconds, which is up to 2/3 of the record length. However, only small time lags are of interest, since the coherence time T_c is on the order of a few seconds. The data processor can perform the correlation analysis from shorter record lengths. However, in order to minimize the statistical uncertainty of the correlation function, the record length should be much greater than T_c. The obtained values of T_c for the investigated data records are comparable with those already discussed in the digital analysis.

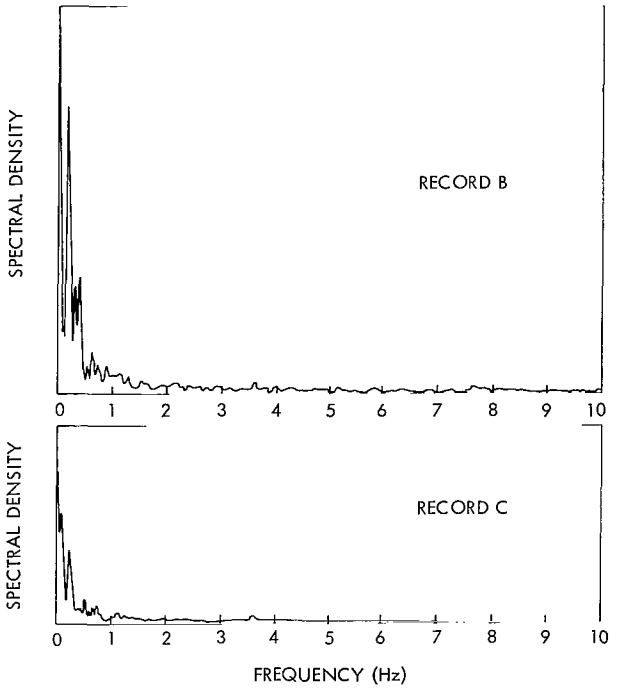

Figure 9—Power spectral density vs. frequency for records B and C.

The spectrum calculation is performed over the 15-Hz analysis range. Again, all records are analyzed and compared with the results of the digital data reduction. Examples for data records B and C are shown in Figure 9.

The record length used for computation in the 15-Hz range is 30 seconds. The resolution bandwidth of the spectrum is 0.0325 Hz. Since all the power spectral densities are derived from data samples, they are statistical estimates of the true spectrum. The latter could be obtained by using certain smoothing and averaging techniques. The ordinate axis in Figure 9 is not calibrated. The derived fading bandwidths of the data records are approximately equal to those obtained in the digital analysis.

The peak at 3.7 Hz, which is present in all of the analog and digital derived power spectral densities, is believed to originate from mechanical resonances of the transmitter antenna.

CONCLUSIONS

The outlined data reduction and experimental data for the short line-of-sight link are a basis for comparison with the data obtained from the ATS-E Millimeter Wave Propagation Experiment. It has been shown that a Rician fading channel is a proper model for a line-of-sight path.

Numerical values for the channel parameters are obtained. The coherence time is on the order of 1.5-4 seconds, and the fading bandwidth is below 0.4 Hz. The main influence of precipitation on wave propagation at 15 GHz is attenuation. No noticeable change of the fading bandwidth due to rain was observed.

It is important that correlation analysis should be performed when the variance of the signal is above a certain threshold (determined by the sensitivity and accuracy of the experiment). As expected, fairly large scintillations of ±1 db are observed during increased windspeeds. The obtained channel parameters (coherence time, fading bandwidth, etc.) could be used for investigating long-term changes. To achieve this, the experiment must be performed over a much longer period (one year).

The estimated maximum scintillation for a link throughout the atmosphere depends on the chosen theoretical model, and can be verified only by an actual measurement. The obtained spectral density of the scintillations for the line-of-sight link are in good agreement with the theoretically derived fluctuation spectra.

ACKNOWLEDGMENT

The author is very indebted to Mr. Erwin Hirschmann for his numerous helpful discussions and critical comments. The assistance given by Messrs. Erwin Hirschmann and Yuichi Otsu in implementing the link and recording the data is gratefully acknowledged.

Goddard Space Flight Center
National Aeronautics and Space Administration
Greenbelt, Maryland, September 9, 1969
125-21-08-06-51

REFERENCES

1. Straiton, A. W., and Tolbert, C. W., "Factors Affecting Earth-Satellite Millimeter Wavelength Communication," *IEEE Trans. Microwave Theory and Techniques,* MTT-11:296-301, September 1963.

2. Altshuler, E. E., Falcone, V. I., and Wulfsberg, K. N., "Atmospheric Effects on Propagation at Millimeter Wavelengths," *IEEE Spectrum,* 5:83-90, July 1968.

3. Hogg, D. C., "Path Diversity in Propagation of Millimeter Waves Through Rain," *IEEE Trans. Antennas and Propagation,* AP-15:410-415, May 1967.

4. Blevis, B. C., Dohoo, R. M., and McCormick, K. S., "Measurement of Rainfall Attenuation at 8 and 15 GHz," *IEEE Trans. Antennas and Propagation,* AP-15:394-403, May 1967.

5. Bello, P. A., and Nelin, B. D., "The Effect of Frequency Selective Fading on Intermodulation Distortion and Sub-carrier Phase Stability in Frequency Modulation Systems," *IEEE Trans. Commun. Systems,* CS-11:87-101, March 1964.

6. Bello, P. A., and Nelin, B. D., "The Effect of Combined Time and Frequency Selective Fading on the Binary Error Probabilities in Incoherent Matched Filter Receivers," *IEEE Trans. Commun. Systems,* CS-11:170-186 January 1963, and COM-12:230-231, December 1964.

7. Boorstyn, R. R., and Schwartz, M., "Performance of Analog Demodulators in a Fading Environment," *IEEE Trans. Commun. Theory,* COM-16:45-51, February 1968.

8. Bello, P. A., "Characterization of Randomly Time-Variant Linear Channels," *IEEE Trans. Commun. Systems,* CS-11:360-393, December 1963.

9. Gallager, R. G., "Characterization and Measurement of Time- and Frequency-Spread Channels," MIT, Lincoln Lab., Technical Report 352, April 1964.

10. Bendat, J. S., and Piersol, A. G., "Measurement and Analysis of Random Data," New York: John Wiley and Sons, 1966.

11. Hogg, D. C., "Millimeter-Wave Communication through the Atmosphere," *Science* 159:39-46, January 1968.

12. Gunn, K. L. S., and East, T. W. R., "The Microwave Properties of Precipitation Particles," *J. Roy. Meteorol. Soc.,* 80:522-545, 1954.

13. Medhurst, R. G., "Rainfall Attenuation of Centimeter Waves: Comparison of Theory and Experiment," *IEEE Trans. Antennas and Propagation,* AP-13:550-564, July 1965.

14. Schwartz, M., Bennett, W. R., and Stein, S., "Communication Systems and Techniques," New York: McGraw-Hill, 1966.

15. Mondre, E., "Relationship between Complex and Envelope Covariance for Rician Fading Communication Channels," NASA Technical Note D-4825, November 1968.

16. Schwartz, M., "Information Transmission, Modulation, and Noise," New York: McGraw-Hill, 1959.

17. Tatarski, V. I., "Wave Propagation in a Turbulent Medium," New York: McGraw-Hill, 1961.

18. Tatarski, V. I., "Fluctuations in Line-of-Sight Propagation of Electromagnetic Waves," in: *Atmospheric Turbulence and Radio-Wave Propagation,* International Colloquium, Moscow, USSR, June 15-22, 1965.

19. Lane, J. A., "Small-Scale Variations of Radio Refraction Index in the Troposphere," *Proc. IEE,* 115:1227-1234, September 1968.

20. Ippolito, L. J., "Channel Correlation Analysis for the ATS-E Millimeter Wave Experiment," NASA Document X-733-68-339, August 1968.

NASA-Langley, 1970 —— 7

NATIONAL AERONAUTICS AND SPACE ADMINISTRATION
WASHINGTON, D.C. 20546
OFFICIAL BUSINESS

FIRST CLASS MAIL

POSTAGE AND FEES PAID
NATIONAL AERONAUTICS AND
SPACE ADMINISTRATION

"The aeronautical and space activities of the United States shall be conducted so as to contribute . . . to the expansion of human knowledge of phenomena in the atmosphere and space. The Administration shall provide for the widest practicable and appropriate dissemination of information concerning its activities and the results thereof."

—NATIONAL AERONAUTICS AND SPACE ACT OF 1958

NASA SCIENTIFIC AND TECHNICAL PUBLICATIONS

TECHNICAL REPORTS: Scientific and technical information considered important, complete, and a lasting contribution to existing knowledge.

TECHNICAL NOTES: Information less broad in scope but nevertheless of importance as a contribution to existing knowledge.

TECHNICAL MEMORANDUMS: Information receiving limited distribution because of preliminary data, security classification, or other reasons.

CONTRACTOR REPORTS: Scientific and technical information generated under a NASA contract or grant and considered an important contribution to existing knowledge.

TECHNICAL TRANSLATIONS: Information published in a foreign language considered to merit NASA distribution in English.

SPECIAL PUBLICATIONS: Information derived from or of value to NASA activities. Publications include conference proceedings, monographs, data compilations, handbooks, sourcebooks, and special bibliographies.

TECHNOLOGY UTILIZATION PUBLICATIONS: Information on technology used by NASA that may be of particular interest in commercial and other non-aerospace applications. Publications include Tech Briefs, Technology Utilization Reports and Notes, and Technology Surveys.

Details on the availability of these publications may be obtained from:

SCIENTIFIC AND TECHNICAL INFORMATION DIVISION

NATIONAL AERONAUTICS AND SPACE ADMINISTRATION

Washington, D.C. 20546